DOI: 10.1021/cg100055p

CRYSTAL GROWTH & DESIGN Article
2010, Vol. 10
4292–4302

Published as part of a virtual special issue of selected papers presented in celebration of the 40th Anniversary Conference of the British Association for Crystal Growth (BACG), which was held at Wills Hall, Bristol, UK, September 6−8, 2009

First Principles Simulations of the Structural and Dynamical Properties of Hydrated Metal Ions Me^{2+} and Solvated Metal Carbonates (Me = Ca, Mg, and Sr)

Devis Di Tommaso* and Nora H. de Leeuw

Department of Chemistry, University College London, 20 Gordon Street, London, WC1H 0AJ, United Kingdom

Received January 15, 2010; Revised Manuscript Received August 5, 2010

ABSTRACT: The structural and dynamical properties of the alkaline earth metal ions Mg^{2+}, Ca^{2+}, and Sr^{2+} and their carbonate and bicarbonate complexes in aqueous solution are examined through first principles molecular dynamics simulations based on the density functional theory. Calculations were conducted in explicit heavy water molecules and at the average temperature of 400 K, conditions which are necessary to obtain a liquid-like water structure and diffusion time-scales when using gradient corrected density functionals. According to these simulations, the magnesium ion undergoes a significant contraction of its coordination sphere in the $Mg(H)CO_3^{(+)}$ aqueous complex, whereas calcium and strontium increase their average first shell coordination number when coordinated to HCO_3^- or CO_3^{2-}. The analysis of the water exchange processes in the hydration shells of the metals suggests the following order for metal reactivity in solution: $Mg^{2+} < Ca^{2+} < Sr^{2+}$. Moreover, our simulations suggest that the structures of the most stable monomers of magnesium bicarbonate and magnesium carbonate in solution is $Mg[^1\text{-}(H)CO_3](H_2O)_4^{(+)}$; that is, the preferred hydration number is four and the (bi-)carbonate is coordinated to the magnesium in a monodentate mode, whereas the building blocks of $CaCO_3$ in aqueous solutions of calcium bicarbonate and calcium carbonate are $Ca[\eta^1\text{-}(H)CO_3](H_2O)_5^{(+)}$. It is not possible, however, to define a unique building unit for strontium (bi-)carbonate due to the rapid interconversion between the mono- and bi-coordination mode of HCO_3^-, and the spontaneous dissociation of $SrCO_3$ during the simulation period. Molecular dynamics simulations of ion pairs Me^{2+}-X^- (Me = Mg, Ca, and Sr; X = F, Cl, and Br) in water have also been conducted, and the results indicate changes of the structural and dynamical properties of the first and second hydration shell of Mg^{2+} and Ca^{2+}, which are explained in terms of modification by the halide ions of the neighboring water molecules, and consequent "reconstruction" of the first hydration shell of the calcium and magnesium ions.

1. Introduction

The process of homogeneous nucleation of an arbitrary macroscopic crystal of ionic type A_xB_y in an aqueous solution, where A^{a+} are cations and B^{b-} are anions, involves the reaction of the hydrated ions A^{a+} and B^{b-} to form the building units A_xB_y, the clusters $(A_xB_y)_n$, and possibly the critical cluster $[(A_xB_y)_{n*}]$, from which the spontaneous growth of the mineral occurs.[1,2] An accurate knowledge of the solvation structure of the ions A^{a+} and B^{b-} and of their dynamical characteristics is therefore of fundamental importance to our understanding of the nucleation and growth of minerals in solution.

The hydration structure of solvated anions is generally much more flexible than those of cations,[3] and although information regarding their solvation environment is also needed to better understand the reactivity of electrolyte solutions, it is plausible to assume that the process of mineral nucleation is mostly influenced by the chemistry around the metal center. In this respect, solvated metal ions have been the subject of numerous experimental and theoretical studies, and several review papers have summarized the large number of related publications.[4−7]

Magnesium and calcium ions are particularly important in biology and are a key component in natural groundwaters.[8] Moreover, the precipitation of related carbonate minerals, such as calcite ($CaCO_3$), dolomite ($Ca_{0.5}Mg_{0.5}CO_3$), or magnesite ($MgCO_3$), from the reaction of Ca- and Mg-silicate minerals with CO_2 is of particular interest, because it represents the most stable, long-term storage-mechanism for anthropologically generated carbon dioxide.[9] Consequently, understanding the structural and dynamical characteristics of Ca^{2+} and Mg^{2+} in aqueous calcium and magnesium (bi-)carbonate solutions is crucial to determine the factors influencing the rate of precipitation of the calcium and magnesium carbonate phases, and especially any differences between the ions. For example, the formation of $MgCO_3$ is virtually impossible at ambient temperature,[10,11] whereas $CaCO_3$ nucleates spontaneously at room temperature under basic pH conditions.[12]

*Author to whom correspondence should be addressed. E-mail: uccaddi@ucl.ac.uk.

Published on Web 09/01/2010

Molecular dynamics (MD) is a computational technique which is useful for elucidating specific properties that are difficult to measure experimentally,[7] and thus allows the direct exploration of the microscopic behavior of electrolyte solutions, such as the effect of heteroligands or foreign species on the solvation of a metal ion.[13] However, especially for ionic species in aqueous solution, the inclusion of many-body effects in the interaction potentials used in the simulations is crucial if we are to obtain a satisfactory description of the solvated ions.[14,15] Thus, an important contribution to this field is the development of the Car−Parrinello molecular dynamics (CP-MD) technique.[16] In this first principles method, the forces are derived from the electronic structure in the framework of the density functional theory (DFT), which provides the capability to study the role of nonadditivity effects in determining the structure of ion solvation shells.

In this study, we report CP-MD simulations of the hydrated metal cations Mg^{2+}, Ca^{2+}, and Sr^{2+}, and of the corresponding solvated metal bicarbonate and metal carbonate complexes, $MeHCO_3^+$ and $MeCO_3$. This work continues our CP-MD investigation of the dynamical and structural properties of magnesium and magnesium (bi-)carbonate in water,[17] and further aims to compare the hydration structures of Mg^{2+}, Ca^{2+}, and Sr^{2+}, the dominant building units of $Me(H)CO_3^+$ in solution, and the dynamical properties of these solvated alkaline earth metals, since these factors play an important role in the process of crystal nucleation.

The strontium ion does not have the significant biological role of magnesium or calcium. However, the solvation structure of the Sr^{2+}-water solution is of environmental importance due to the β-decaying radioactive contaminant ^{90}Sr (half-life $\approx$ 29 years), which is one of the most abundant radioactive isotopes in groundwater.[18] Moreover, the Sr results would be of interest in a comparison of the behavior of the structural and dynamical properties of the hydrated metal ions and solvated metal (bi-)carbonates when moving down the alkaline earth group.

Finally, we have analyzed in detail the effects of simple halide anions X^- (X = F, Cl, and Br) on the solvation properties of Mg^{2+}, Ca^{2+}, and Sr^{2+} by performing CP-MD simulations of the ion pairs Me^{2+}/X^- in water. This study has been inspired by the recent work by Kowacz and coworkers,[19,20] who showed that the rate of mineral precipitation from aqueous solution can be influenced significantly by simple background electrolytes such as KCl, NaCl, LiCl, NaBr, or NaF.

2. Methodology

2.1. Computational Details. CP-MD simulations were carried out using the CP code included in the Quantum-ESPRESSO package, version 4.0.1.[21] The Perdew−Burke−Ernzerhof (PBE) gradient corrected functional[22] was used to describe the electronic structure because this functional gives a very good description of intermolecular hydrogen bonding,[23,24] along with Vanderbilt ultrasoft pseudopotentials (USPP).[25] The electronic wave functions were expanded in a plane wave (PW) basis set with a kinetic energy cutoff of 30 Ry. The USPP for C, Ca, and Sr was taken from the standard Quantum-ESPRESSO distribution, whereas the USPP for O, H, and Mg were generated using the USPP 7.3 pseudopotential program with a scalar-relativistic calculation.[26] Note that semicore shells were explicitly included for Ca, Mg, and Sr. The accuracy and transferability of these pseudopotentials were tested by comparing the optimized structure and the hydration energies of the hydrated $Me(H_2O)_n^{2+}$ (n = 0−6) clusters obtained using the USPP-PW approach with the results from all-electron and scalar-relativistic calculations using the DMol^3 program[27] (Table SI.1 in Supporting Information). The time step for simulations was set to 0.12 fs and the electronic mass was set to 600 au. All simulations were carried out in the NVT ensemble using a Nosé-Hoover chain thermostat[28] to maintain the average temperature at T = 400 K, which is necessary to obtain a liquid-like water structure and diffusion time scales when using gradient corrected density functionals.[29−31] With regard to the choice of ensemble, NVT simulations are computationally less demanding than the NPT ensemble when running first principles MD simulations using generalized gradient approximation (GGA) density functional, while maintaining good agreement with experiment. In fact, for DFT plane wave MD simulations in the NPT ensemble the convergence of the pressure requires a significantly higher basis set cutoff than can be used for NVT FPMD simulations,[32] thereby leading to a substantial increase in computational time. Another problem, particularly for liquids, is that the equilibration time for NPT dynamics can be significantly larger.[32] The isotopic mass of deuterium was used for hydrogen. For the simulation of the charged systems containing Me^{2+}, Me^{2+}/HCO_3^-, and Me^{2+}/X^- in water (Me = Mg, Ca and Sr; X = F, Cl, Br), calculations have been conducted by implicitly including a homogeneous neutralizing charge density within the computational box.

Scheme 1. Definition of the Possible Coordination Modes of the (Bi-)carbonate Ion to the Metal Ions Mg^{2+}, Ca^{2+}, and Sr^{2+}

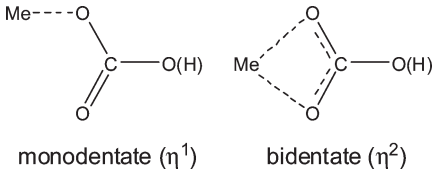

2.2. Simulation Protocol. CP-MD simulations of aqueous solutions of Me^{2+}, $MeHCO_3^+$, and $MeCO_3$ (Me = Mg, Ca, and Sr) have been carried out on a single ion Me^{2+} embedded in a box with 53 water molecules, and on single $MeHCO_3^+$ or $MeCO_3$ species in a box with 52 water molecules. To create the initial configuration, we started from the last configuration of 20 ps of CP-MD simulation on 54 heavy water molecules in a cubic supercell with a side length of 11.94 Å, which corresponds to the extrapolated experimental density of heavy water (D_2O) at 400 K,[29] where one D_2O was replaced by one Me^{2+}. After approximately 2 ps of simulation, the electronic wave function corresponding to the last CP-MD step was reoptimized, and the corresponding structure represented the initial configuration for the simulation of the magnesium, calcium, and strontium in water. For the systems of $MeHCO_3^+$ and $MeCO_3$ in heavy water, we generated the initial configuration by taking a snapshot at approximately 5 ps of the CP-MD simulation of Me^{2+}, and by replacing one D_2O molecule coordinated to the metal ion with one HCO_3^- or CO_3^{2-} ion. Because the (bi-)carbonate can be coordinated to a metal as monodentate (η^1) and bidentate (η^2) (see Scheme 1), for the $MeHCO_3^+$ and $MeCO_3$ species in water, we have conducted two sets of calculations: simulation A, where the initial coordination of $(H)CO_3$ to the metal ions Mg^{2+}, Ca^{2+}, and Sr^{2+} was monodentate and simulation B, where the initial coordination of $(H)CO_3$ to the metals was bidentate.

To generate the initial configuration for the alkali earth metal-halide Me^{2+}/Cl^- (Me = Mg, Ca, and Sr; X = F, Cl, and Br) in aqueous solution, we have first of all conducted a CP-MD simulation where one metal ion was embedded in a cubic supercell with a side length of 13.84 Å with 83 heavy water molecules (the initial configuration was taken from the last snapshot of 6 ps of CP-MD of 84 heavy water molecules, previously generated using a classical molecular dynamics simulation) where one D_2O was substituted by one Me^{2+}. To avoid a situation where the coordination environment around the metal could have been trapped in a local minimum, we initially ran a CP-MD simulation at T = 700 K, followed by 1000 steps at 640, 580, 520, and 460 K. The last configuration of this procedure represented the starting point for the CP-MD simulations at 400 K. Starting from the last configuration of the simulations of Me^{2+} in 83 D_2O, one D_2O at the distance of approximately 5.3 Å from the metal ion was substituted with one X^-.

For all species in aqueous solutions the statistics were then collected for a period of 15−20 ps. The equilibration period was set at 8 ps for Mg^{2+} in 53 water molecules in order to allow the system to go from the initial five-coordinated to the most stable six-coordinated system, whereas for the other systems the equilibration period was set at 4 ps. These calculations required approximately 80000 CPU hours on the "HECToR" and "HPC*x*" UK National Supercomputing Services.

2.3. Characterization of the Dynamics of the Coordination Shells of Me^{2+}. The process of exchange of water molecules between the first and second coordination shells of a metal ion has been quantified using the "direct" method proposed by Hofer and co-workers.[33] In this method, the whole trajectory of the MD simulation is scanned for movements of water molecules, either entering or leaving a coordination shell. Whenever a water molecule crosses the boundaries of this shell, its path is followed and if its new position outside/inside the shell lasts for more than a time parameter t^*, the event is accounted as real. For the time parameter t^* we have chosen the value of 0.5 ps because this has been shown to give a good measure of ligand exchange processes.[33] The mean residence time (MRT) of water molecules in a given coordination sphere is then computed using the following expression:

$$\mathrm{MRT} = \frac{t_{\mathrm{sim}} CN_{\mathrm{av}}}{N_{\mathrm{ex}}} \qquad (1)$$

where t_{sim} is the simulation time, CN_{av} is the average coordination number, and N_{ex} is the number of accounted exchange events.

3. Results and Discussion

3.1. Structure of the Hydrated Me^{2+} and Solvated $MeHCO_3^+$ and $MeCO_3$ (Me = Mg, Ca, and Sr). The influence of the (bi-)carbonate ligand on the coordination spheres of the magnesium, calcium, and strontium ions in aqueous solution can be deduced from the radial distribution functions (RDFs) of the Me−O pairs, $g_{\mathrm{MeO}}(r)$, which are reported in Figure 1 together with the running coordination number $n_{\mathrm{MeO}}(r)$. The value of $n_{\mathrm{MeO}}(r)$ at the first minimum of $g_{\mathrm{MeO}}(r)$ will give, for example, the average number of oxygen atoms which are part of the first coordination shell of Me^{2+}. The relevant data of the first and second peaks of $g_{\mathrm{MeO}}(r)$ are summarized in Table 1, where structural data for $MeHCO_3^+$ and $MeCO_3$ are reported only for the simulations labeled A [monodentate initial coordination of (bi-)carbonate to the metal], as the profiles of the Me-O obtained from simulation B were similar.

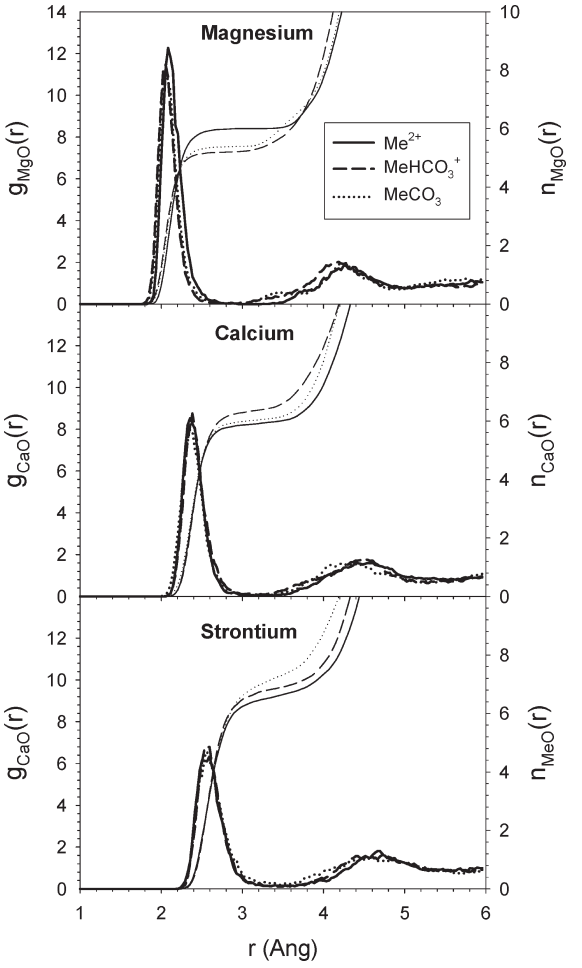

Figure 1. Me-O radial distribution functions, $g(r)$, and running coordination numbers, $n(r)$, for the magnesium, calcium, and strontium metals obtained from the CP-MD simulations labeled A of Me^{2+}, $MeHCO_3^+$, and $MeCO_3$ in water (Me = Mg, Ca, and Sr).

Table 1. Distances $r_{\mathrm{max}}^{\mathrm{MeO}}$ (Å) and Amplitudes $g_{\mathrm{max}}^{\mathrm{MeO}}$ of the Maxima of the First and Second Peak of the Me−O Radial Distribution Functions, and Average Coordination Number CN_{av} of the Respective Shells of the Metal Ions Mg^{2+}, Ca^{2+}, and Sr^{2+}, Obtained from the CP-MD Simulations of Me^{2+}, $MeHCO_3^+$, and $MeCO_3$ in Heavy Water[a]

	$r_{\mathrm{max1}}^{\mathrm{MeO}}$	$g_{\mathrm{max1}}^{\mathrm{MeO}}$	$r_{\mathrm{max2}}^{\mathrm{MeO}}$	$g_{\mathrm{max2}}^{\mathrm{MeO}}$	$CN_{\mathrm{av,1}}$	$CN_{\mathrm{av,2}}$
Mg^{2+}	2.08	12.3 ± 1.2	4.3	1.9	6	12
$MgHCO_3^+$	2.06	11.5 ± 0.6	4.2	2.0	5.2 ± 0.3	13.9
$MgCO_3$	2.06	11.3 ± 1.2	4.2	1.9	5.4 ± 0.4	12.3
Ca^{2+}	2.36	8.5 ± 0.4	4.6	1.6	5.9 ± 0.2	17.0
$CaHCO_3^+$	2.39	8.8 ± 0.5	4.5	1.8	6.4 ± 0.2	15.4
$CaCO_3$	2.36	8.0 ± 0.6	4.4	1.6	$6.0 \pm 3 \times 10^{-2}$	15.8
Sr^{2+}	2.60	6.3 ± 0.7	4.7	1.6	$6.7 \pm 2 \times 10^{-2}$	15.9
$SrHCO_3^+$	2.60	6.3 ± 0.7	4.7	1.6	6.7 ± 0.3	18.1
$SrCO_3$	2.60	6.8 ± 0.3	4.7	1.8	6.9 ± 0.2	19.0

[a] The standard deviations of $g_{\mathrm{max}}^{\mathrm{MeO}}$ and CN_{av} of the first coordination shells of Me^{2+} have been computed from the variation of four block averages within each trajectory.

In general, the Me−H_2O distance and the coordination number increase when moving down the alkaline earth group. The Mg^{2+} ion is characterized by a rigid and very well defined first coordination shell, with the first peak located at 2.08 Å and characterized by a height of 12.3 density units, in agreement with previous CP-MD[34−36] and recent polarizable forcefield MD[37] simulations.

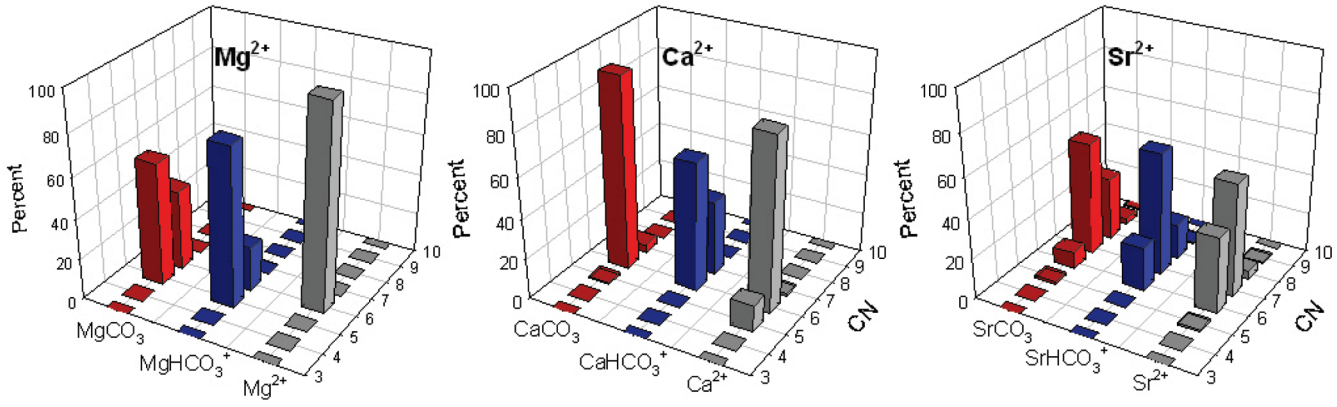

Figure 2. Probability distributions of the coordination numbers of the first coordination shells of the metal ions Mg^{2+}, Ca^{2+}, and Sr^{2+} obtained from the CP-MD simulation of the hydrated Me^{2+}, and of the simulations labeled A of $MeHCO_3^+$ and $MeCO_3$ in water.

For Ca^{2+} in water, the running coordination number at the first minimum of $g_{CaO}(r)$ indicates that the first solvation shell around the ion also has six water molecules, a result fully consistent with previous CP-MD simulations of calcium in water.[34,38,39]

As to the structure of Sr^{2+} in water, the intensity of the first peak of $g_{SrO}(r)$ and the profile of $n_{SrO}(r)$ suggest a less defined first hydration shell for Sr^{2+} than the one for Ca^{2+} and Mg^{2+}. The increase of the average first shell distance (2.6 Å) as well as the corresponding coordination number (6.7) quantifies the expected behavior when moving down the alkaline group. However, experimental studies[40−45] and previous classical[46] and ab initio MD simulations[47−49] suggest a hydration number for Sr^{2+} between 7 and 8. The underestimation of the strontium coordination number by one water molecule is probably related to the simulation temperature of 400 K, which, however, is necessary to obtain a liquid-like behavior when aqueous solutions are simulated using DFT molecular dynamics. In fact, a previous CP-MD simulation of a Sr^{2+} ion solvated by 30 water molecules[47] showed that the running coordination number decreases from 7.6 when the simulation is conducted at 25 °C to 6.7 at 350 °C, in agreement with our results.

The comparison of the Me-O RDFs and the running coordination numbers obtained from the simulations of Me^{2+} and $Me(H)CO_3^+$ shows that for the magnesium ion, the HCO_3^- and CO_3^{2-} anions reduce the coordination sphere of magnesium from an average value of 6 for the hydrated Mg^{2+} to 5.2 and 5.4 for the solvated $MgHCO_3^+$ and $MgCO_3$, respectively (see Table 1). This effect of the HCO_3^- and CO_3^{2-} anions to reduce the magnesium coordination sphere is opposite to the trend observed for Ca^{2+} and Sr^{2+}, where the coordination of the (bi)carbonate increases the size of the coordination sphere of calcium and strontium.

MD is a statistical method and we have therefore attempted to quantify the uncertainties in the computed average values of RDFs and coordination numbers in terms of variation of block averages within each trajectory. Table 1 reports the standard deviations of g_{max}^{MeO} and CN_{av} of the first coordination shells of Me^{2+} computed from four block averages within each CP-MD trajectory. Moreover, the Me-O radial distribution functions and running coordination numbers, together with the square root of the variance of $g(r)$ and $n(r)$, are reported in Figure SI.1 of the Supporting Information.

The effect of the HCO_3^- and CO_3^{2-} anions on the coordination shell of the metals is better appreciated in Figure 2, where we report the probability distributions of the first coordination shell of the metal ions obtained from the simulations labeled A. The graphs indicate that only five- and six-coordinated Mg species are present in solution. The hydrated Mg^{2+} is six-coordinated throughout the simulation period used to gain statistics, whereas the population of 5-coordinated species significantly increases in the aqueous magnesium bicarbonate (78%) and magnesium carbonate (60%) complexes. For the calcium ion, the population of 5-coordinated species, which is approximately 15% for the isolated calcium ion in solution, is negligible in the calcium (bi-)carbonate solutions, whereas the population of seven-coordinated calcium complexes increases in the aqueous calcium(bi-)carbonate complexes. Similarly, the percentage of eight-coordinated strontium species in solution increases from just 4% in the solution of Sr^{2+}, to 18 and 31% in the solutions containing the Sr^{2+}/HCO_3^- and Sr^{2+}/CO_3^{2-} heteropairs, respectively. These results are supported by the probability distributions obtained from the set of simulations labeled B, which are reported in the Supporting Information (Figure SI.2).

To determine the structure of the building units of $MeHCO_3^-$ and $MeCO_3$ in solution, that is, the number of water molecules which are part of the first coordination shell of the metal and the dominant coordination mode of the (bi-)carbonate, we have decomposed the Me−O radial distribution function into the water oxygen atoms (O_w) [$g_{MeOw}(r)$] and the (bi-)carbonate oxygen atoms (O_c) [$g_{MeOc}(r)$] contributions.

For $MgHCO_3^+$ in water, the average coordination numbers $n_{MgOw}(r)$ and $n_{MgOc}(r)$ of the first shell of Mg^{2+} obtained from the simulations labeled A and B are close to 4 and 1, respectively (see Figure 3). This indicates that the magnesium−bicarbonate pair in solution exist almost uniquely as $Mg[\eta^1\text{-}HCO_3](H_2O)_4^+$. As to the structure of $MgCO_3$ in solution, the Mg−O_w and Mg−O_c RDFs, which are reported in Figure 4, show that the average water coordination number as well as the most stable coordination mode of the carbonate to Mg^{2+} depends on the initial conformation of the magnesium−carbonate complex. For simulation A, where the coordination of the CO_3^{2-} to the magnesium was initially monodentate, the values of the running coordination number $n_{MgOw}(r)$ and $n_{MgOc}(r)$ at the first minimum of their respective radial distribution functions is 4.1 and 1.0, respectively. However, from simulation B we obtain an average coordination number of 3.7 for the Mg−O_w pair and 2.0 for the Mg−O_c pair. This suggests that in aqueous solution the CO_3^{2-} anion can be both mono- and bicoordinated to the magnesium atom. However, the average total energy of the system $MgCO_3$ in water

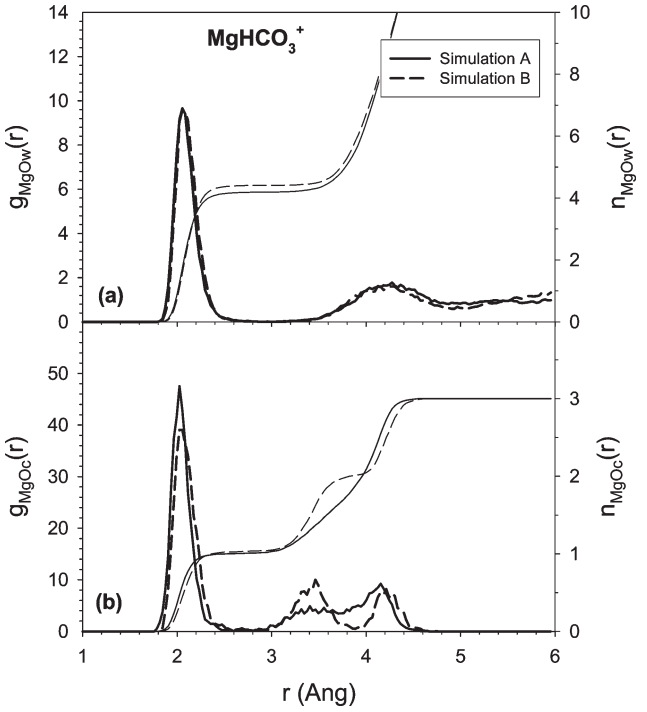

Figure 3. (a) Mg−O_w and (b) Mg−O_c radial distribution functions, $g(r)$, and running coordination numbers, $n(r)$, obtained from the CP-MD simulations of $MgHCO_3^+$ in water. In simulation A, the initial coordination of HCO_3^- to the magnesium was monodentate (η^1); in simulation B, the initial coordination of HCO_3^- to the magnesium was bidentate (η^2).

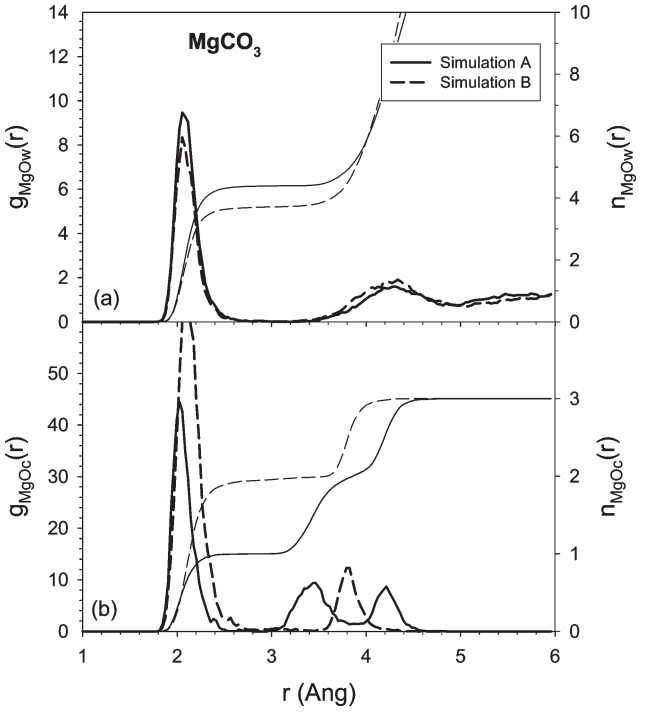

Figure 4. (a) Mg−O_w and (b) Mg−O_c radial distribution functions, $g(r)$, and running coordination numbers, $n(r)$, obtained from the CP-MD simulations of $MgCO_3$ in water. In simulation A the initial coordination of CO_3^{2-} to the magnesium was monodentate (η^1); in simulation B the initial coordination of CO_3^{2-} to the magnesium was bidentate (η^2).

obtained from simulation A (−989.47968 ± 0.03074 au), where the dominant species in solution is Mg(η^1-CO_3)$(H_2O)_4$,

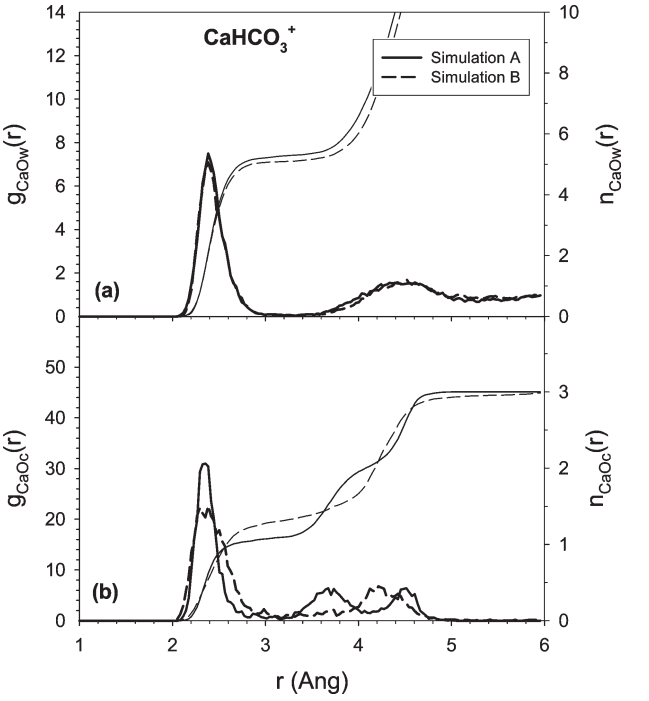

Figure 5. (a) Ca−O_w and (b) Ca−O_c radial distribution functions, $g(r)$, and running coordination numbers, $n(r)$, obtained from the CP-MD simulations of $CaHCO_3^+$ in water. In simulation A, the initial coordination of HCO_3^- to the calcium was monodentate (η^1); in simulation B, the initial coordination of HCO_3^- to the calcium was bidentate (η^2).

is approximately 20 kcal mol^{-1} lower than the average total energy obtained from simulation B (−989.444801 ± 0.033312 au), which is by far larger than the thermal energy at 400 K (kT = 0.79 kcal/mol). Therefore, the η^1-coordination species is by far the most stable $MgCO_3$ complex in solution. This result is also supported by calculations of the solvation free energy of Mg$(CO_3)(H_2O)_4$ using a polarizable dielectric continuum model to simulate an aqueous environment, which has shown that Mg(η^1-CO_3)$(H_2O)_4$ is 9 kcal mol^{-1} more stable than the Mg(η^2-CO_3)$(H_2O)_4$ species.[17]

In Figure 5, the running coordination numbers $n_{CaOw}(r)$ and $n_{CaOc}(r)$ at the first minimum of the Ca−O_w and Ca−O_c suggest Ca(η^1-HCO_3)$(H_2O)_5$ as the dominant building block, that is, the preferred hydration number is five while the (bi-)carbonate is coordinated to the calcium in a monodentate mode. Similar to what was observed for $MgCO_3$, the structural characterization of $CaCO_3$ in solution, which is reported in Figure 6, indicates that calcium−carbonate can exist as Ca[η^1-CO_3] and Ca[η^2-CO_3], with 4−5 water molecules coordinated, on average, to the calcium metal center. This time, the average total energy of the solution where the calcium carbonate monomer is mostly Ca[η^1-CO_3] (simulation A) is only ∼2.5 kcal mol^{-1} lower than the solution where Ca[η^2-CO_3] is the stable species for most of the simulation (simulation B). This small energy difference indicates a facile interconversion between the η^1 and η^2 calcium−carbonate aqueous complexes, which is in fact observed during the ab initio MD simulations (Figure SI.3 in Supporting Information). Moreover, for the simulation of $CaCO_3$ in water labeled A, the analysis of the time windows corresponding to the monodentate (4−16 ps) and bidentate (16−22 ps) coordination modes shows that the average Kohn−Sham energy in the 4−16 ps time frame (−987.347644 ± 0.02635 au)

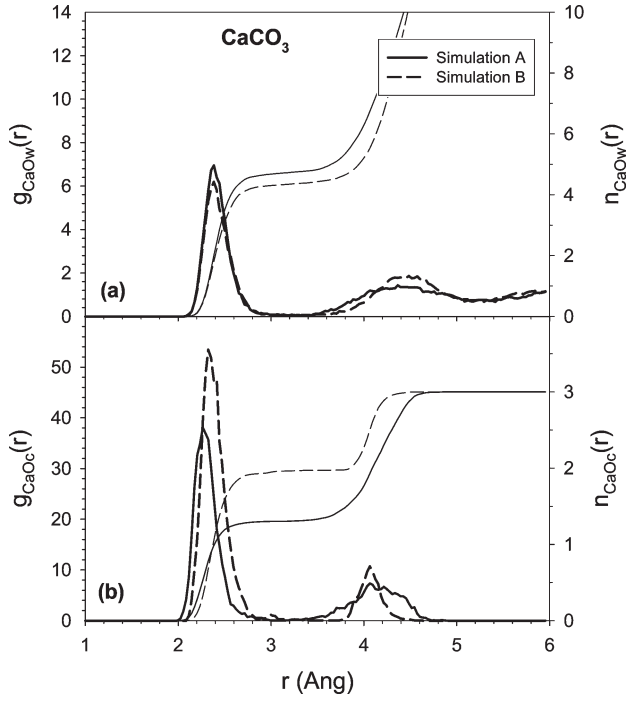

Figure 6. (a) Ca−O_w and (b) Ca−O_c radial distribution functions, $g(r)$, and running coordination numbers, $n(r)$, obtained from the CP-MD simulations of $CaCO_3$ in water. In simulation A, the initial coordination of CO_3^{2-} to the calcium was monodentate (η^1); in simulation B, the initial coordination of HCO_3^{2-} to the calcium was bidentate (η^2).

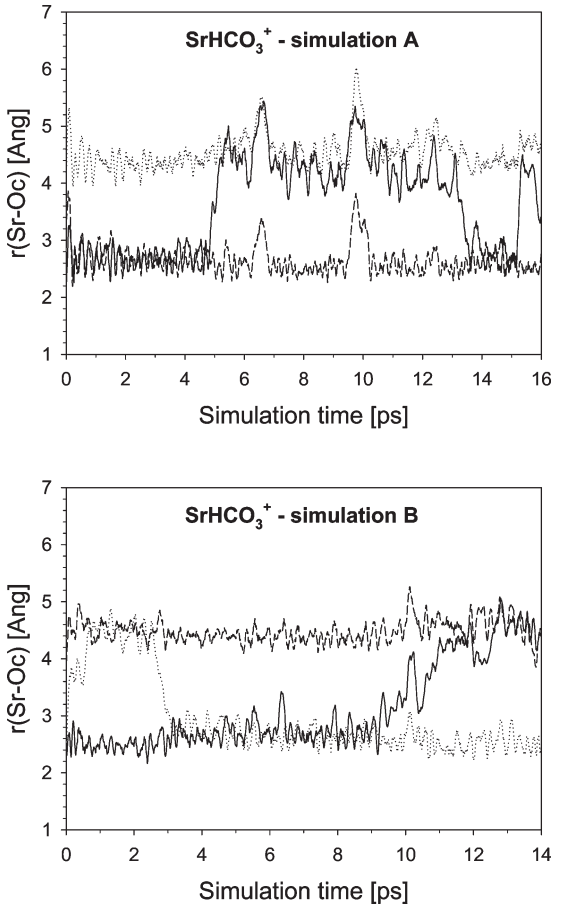

Figure 7. Time evolution of Sr−O distances for the oxygen atoms of the bicarbonate ion. In simulation A, the initial coordination of HCO_3^- to the strontium was monodentate (η^1); in simulation B, the initial coordination of HCO_3^- to the strontium was bidentate (η^2).

is 11.5 kcal/mol lower than the average Kohn−Sham energy of the 16−22 ps time frame (−987.32951 ± 0.03459 au). This indicates that within the same trajectory, the configurations in which CO_3^{2-} is monocoordinated to Ca^{2+} are considerably more stable than those in which CO_3^{2-} is bicoordinated to Ca^{2+}. However, it is also necessary to notice that to evaluate the relative stability of the η^1- and η^2-CO_3 coordination modes it would be necessary to compute the free energy differences between these two states using appropriate free energy sampling methods.

The time evolution of the Sr−O_c distance in $SrHCO_3^+$ in Figure 7 shows the occurrence of several interconversions between the η^1 and η^2 coordination modes. Because of the limit of current computing resources, Figures 7 and 8 indicate that the sampling for the Sr systems is incomplete as many oscillations between states are needed to obtain correctly weighted distribution. Our conclusions for the structural properties of the solvated Sr^{2+}-HCO_3^- and Sr^{2+}-CO_3^{2-} complexes are therefore more qualitative than quantitative with regard to the comparison of the different coordination modes of HCO_3^- to Sr^{2+}.

In Figure 8, the time evolution of the Sr−O_c for the solvated $SrCO_3$ indicates that $SrCO_3$ dissociates after only 12 ps from the start of the simulation, probably as a consequence of the increased "lability" of the coordination shell when moving down the group. In this respect, notice that our results have a resemblance to the experimental speciation results of the complexes $MgCO_3$, $CaCO_3$, and $SrCO_3$. In fact, at 300 K the dissociation constants of $CaCO_3$ and $MgCO_3$ complexes are 3.98×10^{-4} and 6.31×10^{-4},[50] respectively, whereas the dissociation constant of $SrCO_3$ is estimated at 1.86×10^4.[51]

3.2. Dynamics of the Hydrated Me^{2+} and Solvated $MeHCO_3^+$ and $MeCO_3$. Ligand exchange between coordination shells around metal ions in aqueous solution is essential if these ions are to react.[52] In this respect, the exchange processes between hydration shells of metal ions are the most common and important ligand substitution in a solvated metal.[7] Therefore, to quantify the dynamics of the solvation shells of the hydrated metal ions Mg^{2+}, Ca^{2+}, and Sr^{2+} and the effect of the (bi-)carbonate ligand on the reactivity of these metals in solution, we have computed the number of exchange events of the water molecules ($N_{ex}^{H_2O}$) in the first and second coordination shells of the metals during the CP-MD simulations of the hydrated Me^{2+} and of the solvated $Me(H)CO_3^{(+)}$.[33] Table 2 reports $N_{ex}^{H_2O}$ in the first and second coordination shells of the metal ions, together with the number of exchange events normalized to 10 ps, $N_{ex}^{H_2O}/10$, which is a measure of the "lability" of the hydration shell of the metal,[33] and the mean residence time (MRT) of water molecules in the solvation shells.

The number of exchange events in the first hydration shell of Me^{2+} increases on going from Mg^{2+} to Ca^{2+} and Sr^{2+} (see Table 2), which suggests that the reactivity of these metals in solution varies as follows: $Mg^{2+} < Ca^{2+} < Sr^2$.

Moreover, the effect of coordination of the (bi-)carbonate on the dynamics of the first hydration shell of the metals is not certain. For $MgCO_3$ and $MgHCO_3^+$, the water exchange events are only 1 or 2 per simulation, and it is therefore impossible to draw any statistical conclusion from such small numbers. The same applies for the calcium-(bi)carbonate

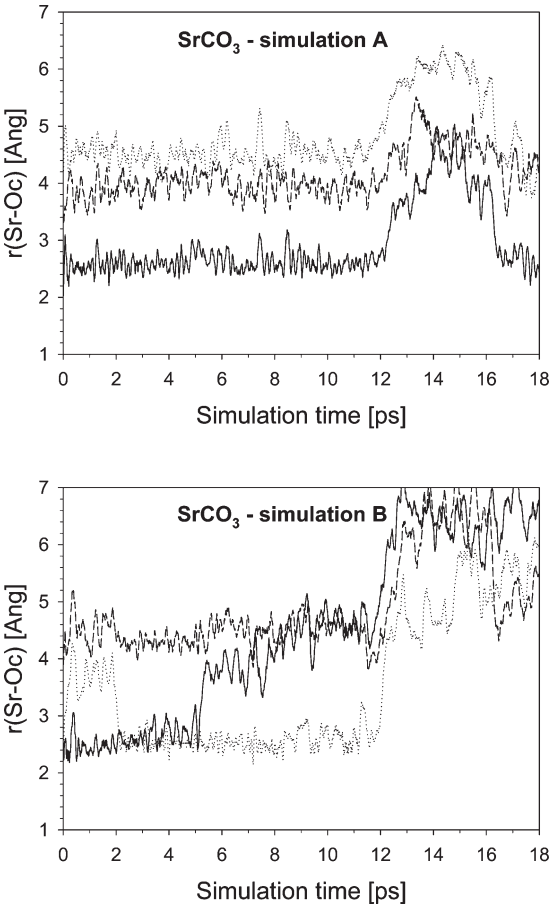

Figure 8. Time evolution of Sr−O distances for the oxygen atoms of the carbonate ion. In Simulation A the initial coordination of CO_3^{2-} to the strontium was monodentate (η^1); in simulation B the initial coordination of CO_3^{2-} to the strontium was bidentate (η^2).

complexes. For example, the MRT of the first hydration shell of the calcium ion does not change significantly on going from the Ca^{2+}-aqueous complex (23.2 ps) to the aqueous calcium-bicarbonate solution labeled A (16.5 ps), whereas the computed MRT from simulation B increases by a factor of 4 (92.8 ps). The opposite situation occurs for the $CaCO_3$, where simulation A predicts a MRT of 117.0 ps, that is, five times higher than the one computed for the Ca^{2+}-aqueous complex, whereas from simulation B the MRT changes from 23.2 to only 37.4 ps (see Table 2). As to the dynamics of the second hydration shell, the numbers of the exchange events are large enough to draw a conclusion on how a (bi-)carbonate ligand affects the hydration dynamics of Me^{2+}: the MRT of water molecules computed for the second hydration shell are in the range of 3.3−4.0 ps (Table 2) which generally increase for the solvated $Me(H)CO_3^{(+)}$, especially for Mg and Ca, indicating that the HCO_3^- and CO_3^{2-} ligands "stabilize" the second coordination shell of the cations.

The radii of the second hydration shells of these metal ions are close to half the length of the simulation box. In order to verify if the system size and periodicity has affected the values of MRTs, we have computed the number of water exchange events in the hydration shells of magnesium, calcium, and strontium obtained from the CP-MD simulations of the metal ions Me^{2+} in 53 and 83 water molecules. The results are reported in Table SI.2 of the Supporting Information and show consistent values of MRTs for both first and second hydration shells.

Table 2. Number of Accounted *water* Exchange Events ($N_{ex}^{H_2O}$) in the First and Second Coordination Shells of the Magnesium, Calcium, and Strontium Atoms, with a Duration of More than $t > t^*$ ($t^* = 0.5$ ps), Obtained from the CP-MD Simulations of Me^{2+}, $MeHCO_3^+$, and $MeCO_3$ in Water ($Me^{2+} = Mg^{2+}$, Ca^{2+}, and Sr^{2+})[a]

	t_{sim} (ps)	CN_{av}	$N_{ex}^{H_2O}$	$N_{ex}^{H_2O}$/ 10 ps	MRT (ps)
	First Shell				
Mg^{2+}	20.5	6	0	0	
$MgHCO_3^+$ (simulation A)	19.7	5.2	1	0.5	102.4
$MgHCO_3^+$ (simulation B)	16.4	5.4	2	1.2	44.2
$MgCO_3$ (simulation A)	22.6	5.4	1	0.4	122.0
$MgCO_3$ (simulation B)	23.4	5.7	2	0.9	66.7
Ca^{2+}	19.3	6.0	5	2.6	23.2
$CaHCO_3^+$ (simulation A)	15.5	6.4	6	3.1	16.5
$CaHCO_3^+$ (simulation B)	14.5	6.4	1	0.1	92.8
$CaCO_3$ (simulation A)	19.5	6.0	1	0.1	117.0
$CaCO_3$ (simulation B)	17.8	6.3	3	1.7	37.4
Sr^{2+}	17.3	6.7	15	8.7	7.7
$SrHCO_3^+$ (simulation A)	14.7	6.7	10	6.8	9.8
$SrHCO_3^+$ (simulation B)	15.4	7.0	14	9.1	7.7
$SrCO_3$ (simulation A)	16.8	6.9	16	9.5	7.2
$SrCO_3$ (simulation B)	15.7	6.6	13	8.3	8.0
	Second Shell				
Mg^{2+}	20.5	12.0	61	29.8	4.0
$MgHCO_3^+$ (simulation A)	19.7	13.9	55	27.9	5.0
$MgHCO_3^+$ (simulation B)	16.4	12.6	34	20.7	6.1
$MgCO_3$ (simulation A)	22.6	12.3	45	19.9	6.2
$MgCO_3$ (simulation B)	23.4	13.0	84	35.9	3.6
Ca^{2+}	19.3	17.0	86	44.6	3.8
$CaHCO_3^+$ (simulation A)	15.5	15.4	49	31.6	4.9
$CaHCO_3^+$ (simulation B)	14.5	13.9	75	51.7	2.7
$CaCO_3$ (simulation A)	19.5	15.8	56	28.7	5.5
$CaCO_3$ (simulation B)	17.8	15.0	44	24.7	6.1
Sr^{2+}	17.3	17.9	94	54.3	3.3
$SrHCO_3^+$ (simulation A)	14.7	18.1	66	44.9	4.0
$SrHCO_3^+$ (simulation B)	15.4	18.9	91	59.1	3.2
$SrCO_3$ (simulation A)	16.8	19.0	42	25.0	7.6
$SrCO_3$ (simulation B)	15.7	16.0	69	43.9	3.6

[a] The first and second coordination shells have been defined by the first and second minimum of the Me−O radial distribution functions, respectively.

3.3. Effects of Halide Ions X^- (X = F, Cl, and Br) on the Structure and Dynamics of Hydrated Me^{2+}. We now discuss the effects of the halide ions F^-, Cl^-, and Br^- on the structure and dynamics of the first and second hydration shells of the metals ions Mg^{2+}, Ca^{2+}, and Sr^{2+} in solution. Figure 9 compares the RDFs of the Me-X pairs obtained from the CP-MD simulations of Me^{2+}/X^- in water with the Me−O RDF. The statistical distributions of the halide ions with respect to the hydration shells of the metal show that Mg^{2+} and Ca^{2+} form preferentially nonassociated solvent shared ion pairs (SSHIP) with X^- in solution, $Me^{2+}-OH_2-X^-$, where the cation and anion are separated by one water molecule, and not a contact ion pair (CIP), $Me^{2+}-X^-$.[53] On the other hand, the Sr-X RDFs shows that with Cl^- and F^- the strontium tends to form spontaneously CIPs, whereas the average position of the bromide ion is well outside the first hydration shell of the metal. Recent classical MD simulations of the complexes $Mg-Cl^+$, $Ca-Cl^+$, and $Sr-Cl^+$ in solution[54] and spectroscopic studies of $MgCl_2$[55] and $CaCl_2$ solutions[56] suggest the absence of contact ion pairing between these ions.

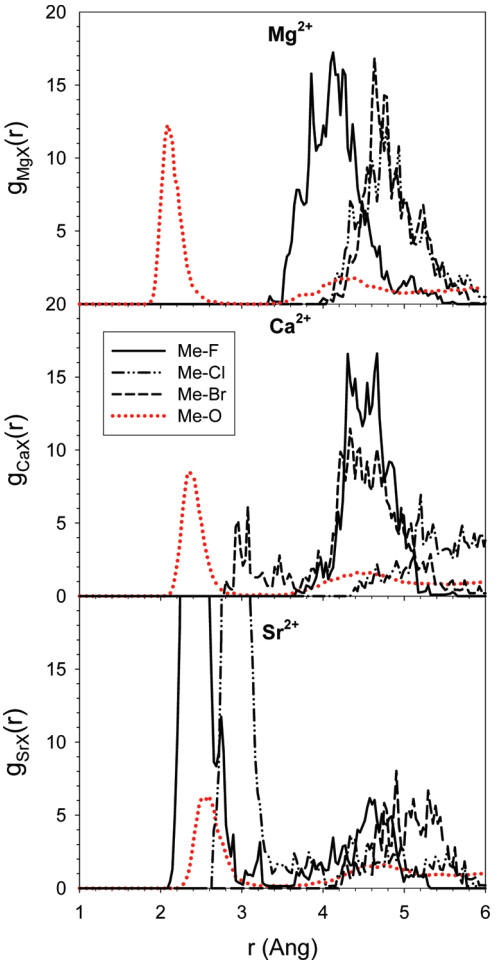

Figure 9. Radial distribution functions, $g(r)$, of the Me-X pairs (Me = Mg, Ca, Sr; X = F, Cl, Br) obtained from the CP-MD simulations of the Me^{2+}/X^{-} pairs in water, and Me-O radial distribution functions (red dotted line) obtained from the CP-MD simulations of Me^{2+} in water.

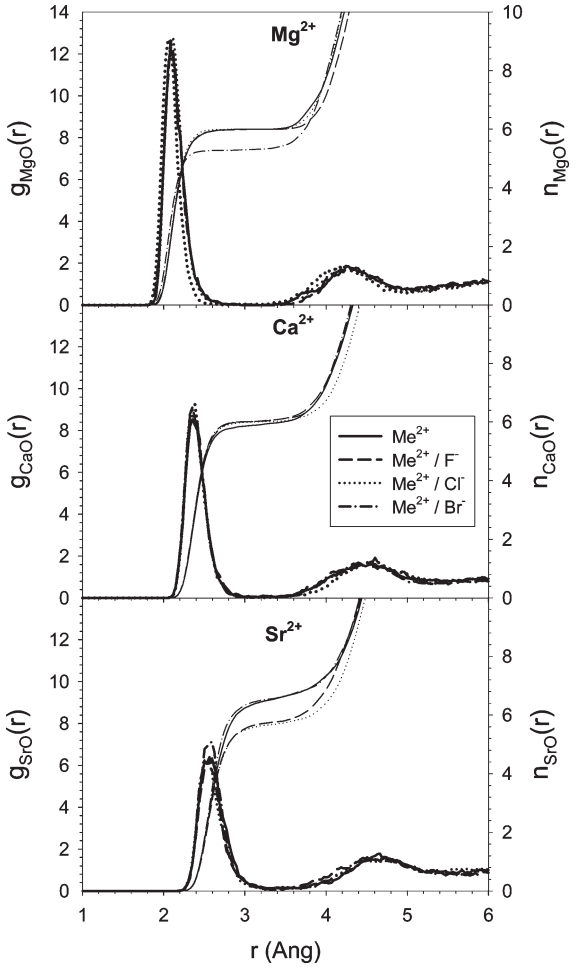

Figure 10. Me-O radial distribution functions, $g(r)$, and running coordination number, $n(r)$, for the magnesium, calcium, and strontium metals obtained from the CP-MD simulations of Me^{2+} in 53 water molecules, and of the nonassociated Me^{2+}/X^{-} in 82 water molecules (Me = Mg, Ca and Sr; X = F, Cl, and Br).

The Me-O RDFs obtained from the solutions containing the halide ions are reported in Figure 10, whereas the most important structural and dynamical parameters of the first and second hydration shells of the metal ions are summarized in Table 3. Starting with the first hydration shell of Mg^{2+}, the presence of chloride and fluoride ions in solution does not influence the position, size, or dynamics of the hydration structure. On the other hand, the bromide anion perturbs the position, as well the size of the hydration shell of Mg^{2+}, which contracts from a stable six coordinated environment to an average value of 5.3 (see Table 3). The dynamical parameters of Mg^{2+} are affected as well, with a significant enhancement of the number of exchange events with respect to either the isolated magnesium ion or the solutions containing F^{-} and Cl^{-}.

The comparison of the Ca−O RDFs obtained from the Ca^{2+}/X^{-} aqueous solutions shows negligible effects on the structural parameters of the first hydration shell of calcium. However, the computed values of the MRTs reported in Table 3 suggest quite strong stabilization, that is, decreased dynamics, of the first hydration shell of Ca^{2+}. In fact, the number of water exchange events goes from the estimated value of 2.6 every 10 ps, to zero exchange events when fluoride or chloride anions are present in solution, and to a just single exchange for the Ca^{2+} in the presence of Br^{-} pair during the 16 ps of simulation.

In solution, the strontium ion spontaneously forms CIPs with F^{-} and Cl^{-} in solution (see Figure 9), which causes a strong stabilization of the solvation shell of Sr^{2+}. In fact, the MRT of water in the first hydration shell of strontium increases from 7.7 ps in the hydrated Sr^{2+} to 16.1 ps in the Sr^{2+}-F^{-} aqueous complex, and to 18.1 ps in the Sr^{2+}-Cl^{-} aqueous complex. The bromide ion is not directly coordinated to Sr^{2+} and they form a SSHIP (see Figure 9), but the value of 16.2 ps for the MRT in the first shell of Sr^{2+} indicates that the presence of Br^{-} ions in solution determines the stabilization of the strontium solvation shell.

Because the halides X^{-} are not directly coordinated to Mg^{2+}, Ca^{2+}, or Sr^{2+} in solution (see Figure 9), the alteration of the structural and dynamical properties of the metals hydration shells has to be explained in terms of modification by the halide ions of their neighboring water molecules.[57] Since metal and halide ions form a SSHIP species in solution, the effect of the halide ions in solution is to "reconstruct" the first hydration shell of calcium, magnesium, and strontium.

As to the second hydration shell, compared with the simulations of the bare cations in water, the values of the MRTs obtained for the solutions containing X^{-} anions

Table 3. Most Important Structural and Dynamical Parameters Obtained from the CP-MD Simulations of the Metal Ions Me^{2+}, and of the Nonassociated Me^{2+}/X^- Pairs in Water (Me^{2+} = Mg^{2+}, Ca^{2+}, and Sr^{2+}; X^- = F^-, Cl^-, and F^-)[a]

	t_{sim} (ps)	r_{max}^{MeO} (Å)	g_{max1}^{MeO}	CN_{av}	$N_{ex}^{H_2O}$/10 ps	MRT (ps)
			First Shell			
Mg^{2+}	20.5	2.08	12.3	6	0	
Mg^{2+}/F^-	17.2	2.08	12.6	6.0	0	
Mg^{2+}/Cl^-	16.9	2.08	12.8	6.0	0	
Mg^{2+}/Br^-	16.7	2.06	12.7	5.3	1.2	44.2
Ca^{2+}	19.3	2.36	8.5	6.0	2.6	23.2
Ca^{2+}/F^-	15.8	2.36	9.2	6.1	0	
Ca^{2+}/Cl^-	16.1	2.38	9.2	6.0	0	
Ca^{2+}/Br^-	15.7	2.36	8.7	6.0	0.6	94.2
Sr^{2+}	17.3	2.60	6.3	6.7	8.7	7.7
Sr^{2+}/F^-	16.7	2.56	6.4	5.8	3.6	16.1
Sr^{2+}/Cl^-	15.9	2.50	6.3	5.7	3.1	18.1
Sr^{2+}/Br^-	14.7	2.60	7.1	6.6	4.1	16.2
			Second Shell			
Mg^{2+}	20.5	4.3	1.9	12.0	29.8	4.0
Mg^{2+}/F^-	17.2	4.3	1.8	11.3	33.1	3.4
Mg^{2+}/Cl^-	16.9	4.2	1.8	11.5	25.4	4.5
Mg^{2+}/Br^-	16.7	4.2	1.8	11.2	29.3	3.8
Ca^{2+}	19.3	4.6	1.6	17.0	44.6	3.8
Ca^{2+}/F^-	15.8	4.6	1.9	15.4	24.1	6.4
Ca^{2+}/Cl^-	16.1	4.6	1.7	15.6	41.0	3.8
Ca^{2+}/Br^-	15.7	4.7	1.5	14.3	34.4	4.2
Sr^{2+}	17.3	4.7	1.6	17.9	54.3	3.3
Sr^{2+}/F^-	16.7	4.6	1.5	17.2	47.3	3.7
Sr^{2+}/Cl^-	15.9	4.6	1.4	15.8	42.8	5.9
Sr^{2+}/Br^-	14.7	4.7	1.6	15.5	40.1	3.9

[a] The first and second coordination shells have been defined by the first and second minimum of the Me−O radial distribution functions, respectively.

suggest that all halogen atoms have the effect of making the second hydration sphere slightly more static.

The results presented in this section therefore suggest that the hydration structure and water dynamics of the first and second hydration shell of metals such as Mg^{2+}, Ca^{2+}, and Sr^{2+} is influenced by the presence of simple anions such as chloride, fluoride, and bromide in the solution. Because the rate of mineral nucleation is critically interconnected with the hydration structure and dynamics of the metals in solution, the results from our simulations indicate that reactivity of metals in solution can be affected by the presence of foreign species, not only through classical mechanisms such as metal complexation but also because of modifications of the solvation environment around the ions involved in the precipitation process.

4. Summary and Conclusions

We have reported a detailed investigation of the structural and dynamical properties of hydrated Me^{2+} ions and of the solvated $MeHCO_3^+$ and $MeCO_3$ complexes in aqueous solution (Me = Mg, Ca, and Sr) using CP-MD simulations.

The structural characteristics of the hydrated magnesium ion and of solvated magnesium (bi-)carbonate complexes indicate that the HCO_3^- and CO_3^{2-} anions reduce the magnesium coordination sphere from a value of 6 to 5.2 and 5.4, respectively, whereas calcium and strontium ions increase their average first shell coordination number when coordinated to HCO_3^- or CO_3^{2-}. The different sizes of the coordination shells of the metals in the building units of $MgCO_3$, $CaCO_3$, and $SrCO_3$ could be one of the factors affecting the very different rates of nucleation of these metal carbonates, which is very slow for magnesite[58] compared to calcium[12] and strontium[59] carbonates.

The dynamics of the metal ions has been quantified in terms of the number of water exchange events in the hydration shells of Mg^{2+}, Ca^{2+}, and Sr^{2+} using the direct method of Hofer et al.[33] The coordination of the (bi-)carbonate ligand leads to a noticeable increase of the "lability" of the magnesium coordination sphere. The results show that the dynamical properties of the first hydration shell of calcium could also be affected by the (bi-)carbonate ligand, but the computed values of the MRT of the first hydration shell of Ca^{2+} depends on the initial configuration of the calcium (bi-)carbonate complex; these discrepancies are attributed to the short period of the CP-MD simulations, associated with the high computational cost of using an ab initio method.

Furthermore, our simulations have been used to characterize the structure of the building units of $MeHCO_3^+$ and $MeCO_3$ in solution. For magnesium- and calcium-bicarbonate aqueous solutions, the monomers are stable as $Mg[\eta^1\text{-}HCO_3](H_2O)_4^+$ and $Ca[\eta^1\text{-}HCO_3](H_2O)_4$, respectively, whereas at basic pH conditions our simulations suggest that both $Me[\eta^1\text{-}CO_3]$ and $Me[\eta^2\text{-}CO_3]$ can be found in solution. However, the average values of the total electronic energies suggest that the $Me[\eta^1\text{-}CO_3]$ complex is the most populated coordination mode.

It is not possible to define a unique building unit for the strontium (bi-)carbonate in water, due to the rapid interconversion between the mono- and bi-coordination modes of HCO_3^-, and the spontaneous dissociation of $SrCO_3$ during the simulation period.

CP-MD simulations of Me^{2+}/X^- pairs (Me = Mg, Ca, Sr; X = F, Cl, F) in water have also been performed. The results show that Ca^{2+} and Mg^{2+} form nonassociated solvent-shared ion pairs with X^-. For Mg^{2+}, the bromide anion perturbs the position, as well the size of the hydration shell of this cation, which contracts from a stable six-coordinated environment to an average value of 5.3. The dynamical parameters of Mg^{2+} are also affected by Br^- in solution, as the number of water exchange events significantly increases with respect to the isolated magnesium ion, or to the solutions containing the Mg^{2+}/F^- and Mg^{2+}/Cl^- pairs. The halide ions also cause quite a strong stabilization, that is, decreased dynamics, of the first hydration shell of Ca^{2+}, with the number of water exchange events going from an estimated value of 2.6/10 ps, to no accounted exchange events when fluoride or chloride anions are in solution, and to just a single exchange for the Ca^{2+}/Br^- solution. A similar stabilization of the metal ion solvation shell is observed in the nonassociated Sr^{2+}/Br^- solution.

The halides X^- are not coordinated to the calcium and magnesium, and their influence on the structural and dynamical properties of the Ca^{2+} and Mg^{2+} in solution has to be explained in terms of modifications by the halide ions of their neighboring water molecules, with consequent reconstruction of the first hydration shell of these metals.

The observed effects of the halide anions on the metal reactivity suggest that the influence of additives to processes of crystal growth and dissolution should be explained not only through processes of metal complexation but also through solvent-mediated effects in the hydration structure of the metal.

Acknowledgment. We acknowledge the EU-funded "Mineral Nucleation and Growth Kinetics (MIN-GRO) Marie-Curie Research and Training Network" for funding (Grant MRTN-CT-2006-035488). Computer resources on the "HPCx" and "HECToR" UK National Supercomputing Services were

provided via our membership with the UK's HPC Materials Chemistry Consortium (Grant No. EPSRC EP/D504872) and Computational Mineral Physics Consortium. We are thankful to the three anonymous referees for all the constructive comments that have helped us to improve the overall quality of our paper.

Supporting Information Available: Tables SI.1 and SI.2; Figures SI.1−SI.3. This information is available free of charge via the Internet at http://pubs.acs.org/.

References

(1) Markov, I. V. *Crystal Growth for Beginners: Fundamentals of Nucleation, Crystal Growth and Epitaxy*, 2nd ed.; World Scientific: Singapore, 2003.

(2) Gebauer, D.; Volkel, A.; Colfen, H. Stable prenucleation calcium carbonate clusters. *Science* **2008**, *322* (5909), 1819–1822.

(3) Rode, B. M.; Schwenk, C. F.; Tongraar, A. Structure and dynamics of hydrated ions-new insights through quantum mechanical simulations. *J. Mol. Liq.* **2004**, *110* (1−3), 105–122.

(4) Marcus, Y. Ionic-radii in aqueous-solutions. *Chem. Rev.* **1988**, *88* (8), 1475–1498.

(5) Ohtaki, H.; Radnai, T. Structure and dynamics of hydrated ions. *Chem. Rev.* **1993**, *93* (3), 1157–1204.

(6) Hofer, T. S.; Randolf, B. R.; Rode, B. M. Computational challenges in simulation methods for liquids and solutions. *AIP Conf. Proc.* **2007**, *963*, 917–920.

(7) Helm, L.; Merbach, A. E. Water exchange on metal ions: experiments and simulations. *Coord. Chem. Rev.* **1999**, *187*, 151–181.

(8) Fraústo da Silva, J. J. R.; Williams, R. J. P. *The Biological Chemistry of the Elements*, 2nd ed.; Oxford University Press: New York, 2001.

(9) Oelkers, E. H.; Gislason, S. R.; Matter, J. Mineral carbonation of CO_2. *Elements* **2008**, *4* (5), 333–337.

(10) Christ, C. L.; Hostetle, P. B. Studies in System MgO-SiO_2-CO_2-H_2O. 2. Activity-product constant of magnesite. *Am. J. Sci.* **1970**, *268* (5), 439–453.

(11) Kittrick, J. A.; Peryea, F. J. Determination of the Gibbs free-energy of formation of magnesite by solubility methods. *Soil Sci. Soc. Am. J.* **1986**, *50* (1), 243–247.

(12) Ogino, T.; Suzuki, T.; Sawada, K. The formation and transformation mechanism of calcium-carbonate in water. *Geochim. Cosmochim. Acta* **1987**, *51* (10), 2757–2767.

(13) Schwenk, C. F.; Rode, B. M. The influence of the Jahn-Teller effect and of heteroligands on the reactivity of Cu^{2+}. *Chem. Commun.* **2003**, *11*, 1286–1287.

(14) White, J. A.; Schwegler, E.; Galli, G.; Gygi, F. The solvation of Na^+ in water: First-principles simulations. *J. Chem. Phys.* **2000**, *113* (11), 4668–4673.

(15) Schwenk, C. F.; Loeffler, H. H.; Rode, B. M. Molecular dynamics simulations of Ca^{2+} in water: Comparison of a classical simulation including three-body corrections and Born-Oppenheimer ab initio and density functional theory quantum mechanical/molecular mechanics simulations. *J. Chem. Phys.* **2001**, *115* (23), 10808–10813.

(16) Car, R.; Parrinello, M. Unified approach for molecular-dynamics and density-functional theory. *Phys. Rev. Lett.* **1985**, *55* (22), 2471–2474.

(17) Di Tommaso, D.; de Leeuw, N. H. Structure and dynamics of the hydrated magnesium ion and of the solvated magnesium carbonates: insights from first principles simulations. *Phys. Chem. Chem. Phys.* *12*, (4), 894−901.

(18) *Some Aspects of Strontium Radiobiology*; Report No. 110; NCRP, National Council on Radiation Protection and Measurements: Bethesda, MD, 1991; p 94.

(19) Kowacz, M.; Prieto, M. R.; Putnis, A. Crystallization and the role of solvent structure dynamics. *Geochim. Cosmochim. Acta* **2009**, *73* (13), A692–A692.

(20) Kowacz, M.; Putnis, A. The effect of specific background electrolytes on water structure and solute hydration: Consequences for crystal dissolution and growth. *Geochim. Cosmochim. Acta* **2008**, *72* (18), 4476–4487.

(21) Giannozzi, P.; Baroni, S.; Bonini, N.; Calandra, M.; Car, R.; Cavazzoni, C.; Ceresoli, D.; Chiarotti, G. L.; Cococcioni, M.; Dabo, I.; Dal Corso, A.; de Gironcoli, S.; Fabris, S.; Fratesi, G.; Gebauer, R.; Gerstmann, U.; Gougoussis, C.; Kokalj, A.; Lazzeri, M.; Martin-Samos, L.; Marzari, N.; Mauri, F.; Mazzarello, R.; Paolini, S.; Pasquarello, A.; Paulatto, L.; Sbraccia, C.; Scandolo, S.; Sclauzero, G.; Seitsonen, A. P.; Smogunov, A.; Umari, P.; Wentzcovitch, R. M. Quantum Espresso: a modular and open-source software project for quantum simulations of materials. *J. Phys.: Condens. Matter* **2009**, *21*, (39), 395502.

(22) Perdew, J. P.; Burke, K.; Ernzerhof, M. Generalized gradient approximation made simple. *Phys. Rev. Lett.* **1996**, *77* (18), 3865–3868.

(23) Zhao, Y.; Truhlar, D. G. Design of density functionals that are broadly accurate for thermochemistry, thermochemical kinetics, and nonbonded interactions. *J. Phys. Chem. A* **2005**, *109* (25), 5656–5667.

(24) Rao, L.; Ke, H. W.; Fu, G.; Xu, X.; Yan, Y. J. Performance of several density functional theory methods on describing hydrogen-bond interactions. *J. Chem. Theory Comput.* **2009**, *5* (1), 86–96.

(25) Vanderbilt, D. Soft self-consistent pseudopotentials in a generalized eigenvalue formalism. *Phys. Rev. B* **1990**, *41* (11), 7892–7895.

(26) http://www.physics.rutgers.edu/∼dhv/ussp/

(27) Delley, B. An all-electron numerical-method for solving the local density functional for polyatomic-molecules. *J. Chem. Phys.* **1990**, *92* (1), 508–517.

(28) Martyna, G. J.; Klein, M. L.; Tuckerman, M. Nose-Hoover chains - the canonical ensemble via continuous dynamics. *J. Chem. Phys.* **1992**, *97* (4), 2635–2643.

(29) Sit, P. H. L.; Marzari, N. Static and dynamical properties of heavy water at ambient conditions from first-principles molecular dynamics. *J. Chem. Phys.* **2005**, *122*, (20), 204510.

(30) Schwegler, E.; Grossman, J. C.; Gygi, F.; Galli, G. Towards an assessment of the accuracy of density functional theory for first principles simulations of water. II. *J. Chem. Phys.* **2004**, *121* (11), 5400–5409.

(31) Fernandez-Serra, M. V.; Artacho, E. Network equilibration and first-principles liquid water. *J. Chem. Phys.* **2004**, *121* (22), 11136–11144.

(32) Schmidt, J.; VandeVondele, J.; Kuo, I. F. W.; Sebastiani, D.; Siepmann, J. I.; Hutter, J.; Mundy, C. J. Isobaric-isothermal molecular dynamics simulations utilizing density functional theory: an assessment of the structure and density of water at near-ambient conditions. *J. Phys. Chem. B* **2009**, *113* (35), 11959–11964.

(33) Hofer, T. S.; Tran, H. T.; Schwenk, C. F.; Rode, B. M. Characterization of dynamics and reactivities of solvated ions by ab initio simulations. *J. Comput. Chem.* **2004**, *25* (2), 211–217.

(34) Ikeda, T.; Boero, M.; Terakura, K. Hydration properties of magnesium and calcium ions from constrained first principles molecular dynamics. *J. Chem. Phys.* **2007**, *127*, (7), 074503.

(35) Lightstone, F. C.; Schwegler, E.; Hood, R. Q.; Gygi, F.; Galli, G. A first principles molecular dynamics simulation of the hydrated magnesium ion. *Chem. Phys. Lett.* **2001**, *343* (5−6), 549–555.

(36) Bernasconi, L.; Baerends, E. J.; Sprik, M. Long-range solvent effects on the orbital interaction mechanism of water acidity enhancement in metal ion solutions: A comparative study of the electronic structure of aqueous Mg and Zn dications. *J. Phys. Chem. B* **2006**, *110* (23), 11444–11453.

(37) Yu, H. B.; Whitfield, T. W.; Harder, E.; Lamoureux, G.; Vorobyov, I.; Anisimov, V. M.; MacKerell, A. D.; Roux, B. Simulating monovalent and divalent ions in aqueous solution using a Drude polarizable force field. *J. Chem. Theory Comput.* **2010**, *6* (3), 774–786.

(38) Bako, I.; Hutter, J.; Palinkas, G. Car-Parrinello molecular dynamics simulation of the hydrated calcium ion. *J. Chem. Phys.* **2002**, *117* (21), 9838–9843.

(39) Lightstone, F. C.; Schwegler, E.; Allesch, M.; Gygi, F.; Galli, G. A first-principles molecular dynamics study of calcium in water. *ChemPhysChem* **2005**, *6* (9), 1745–1749.

(40) Caminiti, R.; Musinu, A.; Paschina, G.; Pinna, G. X-ray-Diffraction study of aqueous Srcl2 solutions. *J. Appl. Crystallogr.* **1982**, *15* (Oct), 482–487.

(41) Moreau, G.; Scopelliti, R.; Helm, L.; Purans, J.; Merbach, A. E. Solution X-ray absorption fine structure study of the Eu^{2+} and Sr^{2+} ions: Unexpected solvent and metal ion dependencies of the solvation numbers. *J. Phys. Chem. A* **2002**, *106* (41), 9612–9622.

(42) Parkman, R. H.; Charnock, J. M.; Livens, F. R.; Vaughan, D. J. A study of the interaction of strontium ions in aqueous solution with the surfaces of calcite and kaolinite. *Geochim. Cosmochim. Acta* **1998**, *62* (9), 1481–1492.

(43) Persson, I.; Sandstrom, M.; Yokoyama, H.; Chaudhry, M. Structure of the solvated strontium and barium ions in aqueous, dimethyl-sulfoxide and pyridine solution, and crystal-structure of strontium and barium hydroxide octahydrate. *Z. Naturforsch., Sect. A* **1995**, *50* (1), 21–37.
(44) Pfund, D. M.; Darab, J. G.; Fulton, J. L.; Ma, Y. J. An XAFS study of strontium ions and krypton in supercritical water. *J. Phys. Chem.* **1994**, *98* (50), 13102–13107.
(45) Steward, T. M.; Henderson, C. M. B.; Charnock, J. M.; Driesner, T. An EXAFS study of solvation and ion pairing in aqueous strontium solutions to 300 °C. *Geochim. Cosmochim. Acta* **1999**, *63* (16), 2409–2418.
(46) Dang, L. X.; Schenter, G. K.; Fulton, J. L. EXAFS spectra of the dilute solutions of Ca^{2+} and Sr^{2+} in water and methanol. *J. Phys. Chem. B* **2003**, *107* (50), 14119–14123.
(47) Harris, D. J.; Brodholt, J. P.; Sherman, D. M. Hydration of Sr^{2+} in hydrothermal solutions from ab initio molecular dynamics. *J. Phys. Chem. B* **2003**, *107* (34), 9056–9058.
(48) Hofer, T. S.; Randolf, B. R.; Rode, B. M. Sr(II) in water: A labile hydrate with a highly mobile structure. *J. Phys. Chem. B* **2006**, *110* (41), 20409–20417.
(49) Tofteberg, T.; Ohrn, A.; Karlstrom, G. Combined quantum chemical statistical mechanical simulations of Mg^{2+}, Ca^{2+} and Sr^{2+} in water. *Chem. Phys. Lett.* **2006**, *429* (4−6), 436–439.
(50) Garrels, R. M.; Thompson, M. E. A chemical model for sea water at 25 °C and one atmosphere total pressure. *Am. J. Sci.* **1962**, *260* (1), 57–66.
(51) Savenko, A. V. Solubilities of strontium carbonate and sulfate in seawater. *Geochem. Int.* **2004**, *42* (2), 178–187.
(52) Richens, D. T. *The Chemistry of Aqua Ions: Synthesis, Structure and Reactivity: A Tour Through the Periodic Table of the Elements*; Wiley: New York, 1997; p 604.
(53) Marcus, Y.; Hefter, G. Ion pairing. *Chem. Rev.* **2006**, *106* (11), 4585–4621.
(54) Larentzos, J. P.; Criscenti, L. J. A molecular dynamics study of alkaline earth metal-chloride complexation in aqueous solution. *J. Phys. Chem. B* **2008**, *112* (45), 14243–14250.
(55) Callahan, K. M.; Casillas-Ituarte, N. N.; Roeselova, M.; Allen, H. C.; Tobias, D. J., Solvation of magnesium dication: molecular dynamics simulation and vibrational spectroscopic study of magnesium chloride in aqueous solutions. *J. Phys. Chem. A 114*, (15), 5141−5148.
(56) Fulton, J. L.; Heald, S. M.; Badyal, Y. S.; Simonson, J. M. Understanding the effects of concentration on the solvation structure of Ca^{2+} in aqueous solution. I: The perspective on local structure from EXAFS and XANES. *J. Phys. Chem. A* **2003**, *107* (23), 4688–4696.
(57) Hribar, B.; Southall, N. T.; Vlachy, V.; Dill, K. A. How ions affect the structure of water. *J. Am. Chem. Soc.* **2002**, *124* (41), 12302–12311.
(58) Saldi, G. D.; Jordan, G.; Schott, J.; Oelkers, E. H. Magnesite growth rates as a function of temperature and saturation state. *Geochim. Cosmochim. Acta* **2009**, *73* (19), 5646–5657.
(59) Li, S.; Zhang, H.; Xu, J.; Yang, D. Hydrothermal synthesis of flower-like $SrCO_3$ nanostructures. *Mater. Lett.* **2005**, *59* (4), 420–422.